



# Improving Energy Harvesting from Cantilever-like Structures Based on Beam Geometry

Polat Kurt<sup>1</sup> · Sadettin Orhan<sup>1</sup>

Received: 19 December 2023 / Revised: 8 February 2024 / Accepted: 22 February 2024  
© The Author(s) 2024

## Abstract

**Purpose** Power gain from piezoelectric harvesters depends on several parameters and one of them is to design the substructure as to increase the mechanical strain occurred in the piezoelectric material. In this study, the effect of geometrical modification of the beam on the harvested power was investigated and new geometries were offered for increased power response from cantilever type energy harvesters.

**Method** First, the effectiveness of auxetic structures on harvested power was investigated to see the effect of the negative Poisson's ratio on harvested power. These structures are very popular in recent years on energy harvesting applications; however, their performances were generally compared to plain structures which is not a fair comparison. Rather, in this study, their performances were compared to non-auxetic nonlinear structures as well as plain geometry. Then, three new shapes inspired by re-entrant auxetic structure were presented for increased power response, and harvested power from these structures were evaluated under different conditions.

**Results** It was shown that the power gain from auxetic structures is very high compared to plain structures; however, this increase in power could also be achieved using a non-auxetic simple rectangular structure in some cases. On the other hand, new geometries offered in this study performed better than the auxetic and non-auxetic geometries in most cases.

**Keywords** Auxetic · Piezoelectric · Energy harvesting · Negative poisson's ratio · Piezoelectric energy harvesters

## Introduction

Piezoelectric energy harvesting has been widely studied in recent years as a method to convert otherwise dissipated mechanical energy into useful electrical energy. One of the notable advantages of piezoelectric energy harvesting is its versatility in various applications. It can be integrated into a wide range of systems, from small-scale wearable devices to large-scale infrastructure, or dynamic systems to capture ambient vibrations and convert them into usable electrical power [1–5]. Typical energy harvesters generally consist of a substructure and piezoelectric material bonded to it, and produce electrical energy by converting the applied mechanical energy [6]. The harvested power from these structures, however, is in low ranges and needs to be improved. Numerous studies have investigated different parts of the energy

production steps to improve electrical power generation. The first thing that comes to mind is to improve the properties of piezoelectric materials. Roscow et al. [7] proposed porous piezoelectric materials with increased energy harvesting figures of merit. It was shown that the porosity in the material increases the piezoelectric strain constant and decreases the permittivity, thereby increasing the power gain. In another study, Szweczyk et al. [8] improved the conditions in electrospinning of PVDF (Polyvinylidene fluoride) and showed that piezoelectric constant of PVDF can be increased by controlling certain parameters in this stage. Zhang et al. [9] produced BCZT ( $\text{Ba}_{0.85}\text{Ca}_{0.15}\text{Zr}_{0.1}\text{Ti}_{0.9}\text{O}_3$ ) ceramics with large grain sizes using the sol-gel method. They obtained excellent piezoelectric properties. Ongun et al. [10] enhanced the piezoelectric properties of PVDF by using graphene oxide and reduced graphene oxide additives to increase the electrical output. On the other hand, many studies [11–13] have worked on electrical impedance matching for external circuits and piezoelectric materials to optimize the harvested energy. The main idea here was to minimize the electrical energy loss in the electrical energy

✉ Polat Kurt  
polatkurt@aybu.edu.tr

<sup>1</sup> Department of Mechanical Engineering, Ankara Yıldırım Beyazıt University, Ankara, Turkey

production step by matching the electrical impedances of the external circuit and the piezoelectric material. Another method to boost the harvested energy is to design the substructure to increase the mechanical energy therefore the electrical energy. One of the recent boosting methods for power gain is the use of auxetic structures in the design of substructures [14]. Normally, most materials shrink in the lateral direction when stretched in the longitudinal direction because of the positive Poisson's ratio [15]. Classical energy harvesters exposed to bending forces produce energy using the strain that occurs in the longitudinal direction and convert it into electrical energy with the help of piezoelectric constants of piezoelectric material. This is because conventional beam shapes have positive Poisson's ratios. On the other hand, auxetic-shaped beams have a negative Poisson's ratio, and therefore, strains that occur in the longitudinal and lateral directions have the same sign [16].

To increase the harvested energy, designing beam structure is one of the most used methods. For instance, Ravanbod and Nejad [17] worked on a meta-structure booster for energy harvesters and the power was increased by 15 times compared to a plain harvester. A novel hybrid tri-stable energy harvester was implemented to improve the efficiency of energy harvesters by Dawei et al. [18]. Silveira and Daniel [19] performed an optimization work based on number of harvesters and the geometry of them. They assembled the harvesters on a tilting pad bearing and they have increased the power gain nearly 35%. Numerous studies have been conducted using auxetic geometries in substructures for piezoelectric energy harvesting applications. Ferguson et al. [20] studied energy harvesting using a substructure with a re-entrant design under oscillatory strain excitation in the longitudinal direction. It was shown that 191.1  $\mu\text{W}$  of energy was harvested under 250  $\mu\text{S}$  strain when the auxetic shape was used, and this value was 14.4 times higher than the power harvested by a non-auxetic harvester. Chen et al. [21] used the same type of auxetic structure; however, they used the bending motion of the structure instead of the longitudinal one and applied a 0.1 g base excitation to the cantilever-type harvester. The power gain was 173% higher than that of the plain-shaped harvesters. Eghbali et al. [22] proposed a circular auxetic structure and used it as a substructure for energy harvesters. They found that the power magnification factor was 10 times that of plain-type harvesters. Sadikbasha et al. [23] studied hexachiral structures and proposed a single-degree-of-freedom semi-analytical model for voltage gain from these structures. The results were validated using the finite-element method and experiments. Their harvesters outperformed the previously introduced models with a power gain 10 times that of the plain and three times that of the re-entrant structure. There are different auxetic designs offered in the literature with different power increases compared to plain harvesters [24–27].

The use of auxetic structures may seem highly advantageous in energy harvesting applications compared to plain harvesters, however, this can be misleading because same increase in energy can be achieved also by using non-auxetic, nonlinear structures. Therefore, the use of auxetic structures for piezoelectric energy harvesting should be studied further and the benefits of the structures should be compared to the similar non-linear geometries rather than plain structures to see the actual effect of the negative Poisson's ratio. This paper investigates the auxetic structures whether their negative Poisson's ratio highly effective on power response or not and also introduces new non-auxetic geometries that perform better than the auxetic and plain geometries. It consists of 2 case studies each have different conditions. In the first case, different auxetic structures were investigated for their energy harvesting capabilities, and their performances were compared to those of plain beams and non-auxetic nonlinear structures to determine whether the auxetic structures were effective in power generation. For this, two different auxetic structures were used, along with plain and rectangular structures with the same outer dimensions. This case was employed to show the effect of auxetic structures on energy harvesting from transverse vibrations. There are various studies in the literature that shows 10–100 times increase in power response compared to plain structures. However, it is unclear whether it is due to negative Poisson's ratio or frequency change and area reduction in the beam. To show that, average stress and strain values of the auxetic structures were evaluated under different conditions.

In second case, three new structures with higher power gains were also proposed and compared to auxetic structures and plain beam. The analysis was performed by using finite element method and an experimental study was performed in the last part of the study comparing the results to the FEA.

## Material and Method

The amount of energy harvested from vibrating structures through piezoelectricity depends on the properties of the piezoelectric material and the mechanical strain that occurs in the material. For instance, if a cantilever beam with piezoelectric materials bonded on it is excited in the transverse direction, there will be strains in two perpendicular directions acting on the piezoelectric materials (other directions can be omitted). In this case, the open-circuit voltage that can be harvested from piezoelectric materials can be expressed as follows [28]:

$$V = 2 \frac{d_{31}}{\epsilon_{33}^T} (\overline{\sigma}_{11} + \overline{\sigma}_{22}) t = 2 \frac{e_{31}}{\epsilon_{33}^T} (\overline{S}_{11} + \overline{S}_{22}) t \quad (1)$$

where,  $\overline{\sigma}_{11}$  is the average stress in direction-1 and  $\overline{\sigma}_{22}$  is the average strain in the direction-2,  $d_{31}$  is piezoelectric stress constant (assuming  $d_{31} = d_{32}$ ) and  $\epsilon_{33}^T$  is the permittivity

constant and  $t$  is the piezoelectric layer thickness.  $\overline{S_{11}}$  is average strain in  $x$  direction and  $\overline{S_{22}}$  is average strain in  $y$  direction.

For a given load resistance, the power response then can be calculated by

$$P = \frac{V^2}{R} \tag{2}$$

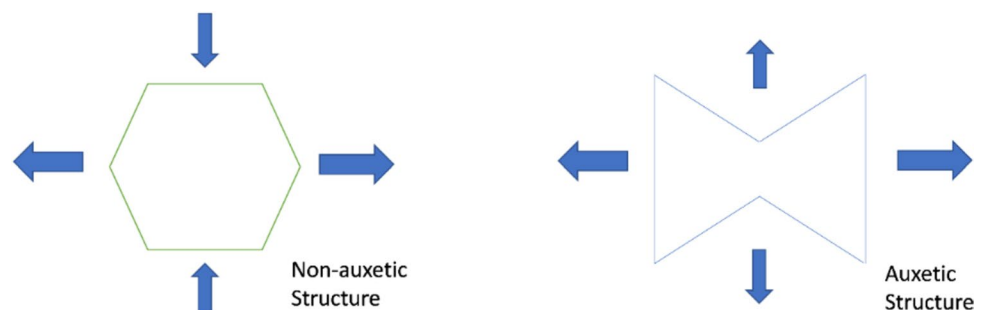
So, it can be said that increasing stresses or strains in  $x$  and  $y$  direction will increase the power response of the piezoelectric materials. For a positive Poisson’s ratio of the substructure, the strains in the first and second directions have opposite signs during vibration. This situation decreases the total strain affecting the piezoelectric material, and therefore, the voltage gain. On the other hand, the strains in perpendicular directions would be of the same sign when auxetic geometries or negative Poisson’s ratio are used for the substructure, and the harvested voltage can theoretically be increased.

Figure 1 shows the behavior of auxetic and non-auxetic structures under loading. It can be seen that stretching in one direction causes shrinking in other directions for non-auxetic structures where the auxetic structure stretches in both directions. If a piezoelectric material was bonded on the auxetic structure, there would be positive strains in two directions. This is the theory, and it is used to improve the power response of the beams comparing them to the plain structures. However, the effectiveness of this phenomenon should be investigated deeply. In the first part of this study, the advantages of this phenomenon in energy harvesting applications were investigated using different auxetic structures proposed in the literature and compared them to non-auxetic geometries using finite element method (FEA). Then, new shapes were offered for increased power response in the second part of the study. The last part includes experimental validation of the performance of some of these structures.

**Finite Element Analysis**

Energy harvesting analysis was implemented by using COMSOL Multiphysics (v5.2a) finite element analysis program along with the SOLIDWORKS (v.2016) modelling software.

**Fig. 1** Auxetic (right) and non-auxetic (left) beams under load



First, a cantilever beam with piezoelectric materials bonded on it was modelled in SOLIDWORKS, as shown in Fig. 2. The model was then transferred to COMSOL using the Live-link Interface between the two programs. The left-hand side of the beam was excited with a prescribed acceleration of 1 g in the  $z$ -direction, while the other side was left free. A commercially available PVDF (MEAS LDT0-028K from TE Connectivity) material was used as piezoelectric materials in the finite element analysis, and two different beam materials were used to compare (Steel and PLA). PVDF was selected due to their availability and affordability in Türkiye. PLA and steel were chosen for their highly different stiffness properties to investigate the effect of energy transfer. The outer dimensions of the beams and the piezoelectric materials used were shown in Fig. 3. All the beams used in the study have the same outer dimensions ( $50 \times 13 \times 3 \text{ mm}^3$ ). These dimensions were chosen according to the PVDF used in the study to fit it into that area. The area under PVDF ( $15 \times 13 \text{ mm}^2$ ) changes in shape to utilize different auxetic and non-auxetic structures. PVDF used in the study consisting of two parts of polyester cover and piezoelectric material itself with dimensions shown in the Fig. 3. Table 1 lists the characteristics of the materials used in this study.

The piezoelectric patches were assumed to be perfectly bonded on the surface of the substructure. The poling direction was controlled by rotating the coordinate axis by  $180^\circ$  in  $Z$  direction to obtain a series connection between materials. The top surface of the upper piezoelectric material was assigned as the terminal surface, and the bottom of the lower piezoelectric material was assigned as the ground.

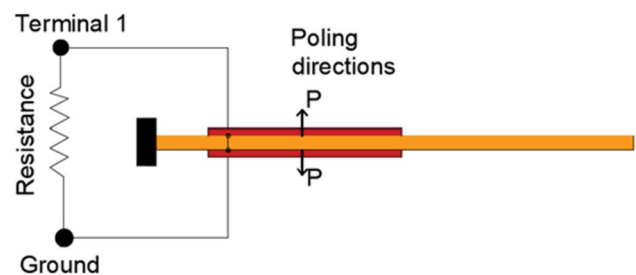


**Fig. 2** Poling directions and resistance connection

**Fig. 3** General dimensions of the harvesters used in the study

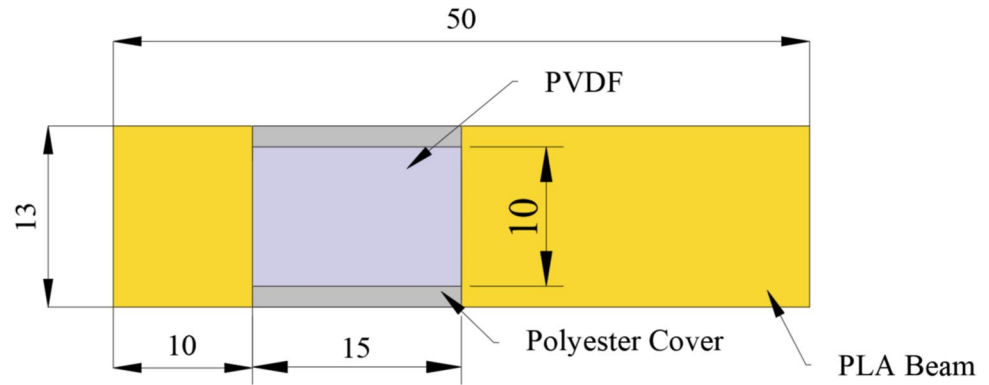


**Table 1** Material properties of materials used in the research

	PLA	Steel	PVDF
Density ( $\text{kg/m}^3$ )	1250	8000	1780
Elasticity in x direction (GPa)	3	200	2.6
Relative Permittivity, $\epsilon_{33}^T/\epsilon_0$	–	–	12
Piezoelectric charge constant— $d_{31}$ , $d_{32}$ (pC/N)	–	–	10
Poisson's ratio	0.3	0.3	

The other two surfaces were assigned as the terminal surfaces. A resistor between the terminal and the ground was created to form a circuit, as illustrated in Fig. 2, and the terminal was selected to measure the electric potential generated by the piezoelectric harvester. An experimental study was performed for two substructures of re-entrant and NS-A geometries which will be defined later. Damping for these substructures were calculated by logarithmic decrement method and imported to the FEA. An average value for stiffness parameter ( $7.4 \times 10^{-5}$ ) of Rayleigh damping was calculated for these substructures and that value was used throughout all the FEA simulations.

After the definitions were completed, an eigenfrequency analysis was made first to determine natural frequencies of the structures. For the given natural frequency, optimum resistance was determined. This value depends on the frequency of the vibration, capacitance of the piezoelectric material and the dimensions of the materials. Therefore, it was evaluated for each case used in the study with parametric sweep for the resistance values under natural frequencies of the harvesters. Finally, frequency response analysis in a range of frequencies were made by using frequency domain analysis type under optimum load resistance value.

In post-processing section, power responses were calculated by using Eq. (2), from Voltage data obtained from piezoelectric materials and optimum resistance values.

## Experimental Verification

The schematic in Fig. 4 depicts the experimental setup for validating the piezoelectric energy-harvesting model. The setup consists of steel and PLA substructures with piezoelectric materials bonded on each side of the beam at the same position. One side of the beam was connected to a shaker while the other side was free. To generate the vibration signal, a function generator was connected to the shaker, and the signal was passed through an amplifier. A Laser Vibrometer (Optomet Nova Speed) was used to measure the acceleration applied to the beam. The piezoelectric materials were connected to each other in series and attached to a resistor to create an external circuit. When the function generator applied a predefined vibration signal to the shaker, the piezoelectric material generated AC voltage. The generated voltage and acceleration signals were sent to an oscilloscope for measurement and analysis. Voltage data was normalized for 1 g of acceleration and then power was calculated from normalized voltage data and resistor used.

## Results and Discussion

The study consists of two cases which include analysis of different structures for their energy harvesting capabilities. In the first case, an investigation on the performances of auxetic structures was performed by using finite element method. Secondly, new shapes offered for increased power response and the performances were compared to the auxetic structures. Finally, some of the structures were experimentally verified.

### Case 1: Effectiveness of Auxetic Structures

This study employed previously suggested auxetic shapes, including re-entrant and anti-tetra-chiral structures, and compared their performances with those of non-auxetic plain and rectangular structures. Figure 5 illustrates the different auxetic and non-auxetic structures used in the

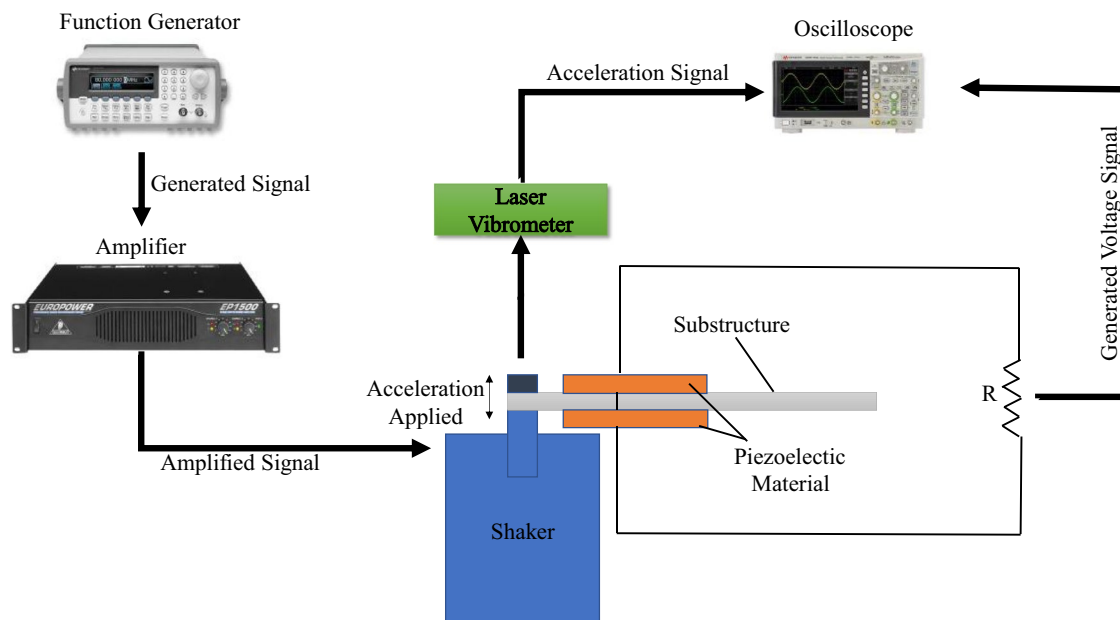


Fig. 4 Experimental set-up for energy harvesting

investigation. The auxetic structures (Fig. 5 a, b) shown in the figure have negative Poisson’s ratio. The others have positive Poisson’s ratio.

This study examined the performance of various beam shapes and piezoelectric materials for harvesting energy across various frequency ranges. First, the optimum resistance values were calculated for each case. Because the maximum power can be harvested at the resonance frequency, the optimum resistance values were calculated at the resonance of the structure. The resonance frequencies and optimum resistance values calculated for the different beams were listed in Table 2.

Results for PLA Beam Case

Figure 6 shows the power responses of PVDF for the different beam geometries and Table 3 shows the maximum harvested power at the natural frequency. Compared to the plain structure, the utilization of auxetic structures has increased the power gain more than 10 times. Maximum power was harvested from re-entrant structure. On the other hand, the power response from the rectangular non-auxetic structure has a maximum power response nearly same that of the anti-tetra-chiral geometry. This indicates that a non-auxetic structure with an area decrease in the geometry can also deliver the power increase achieved by utilizing auxetic

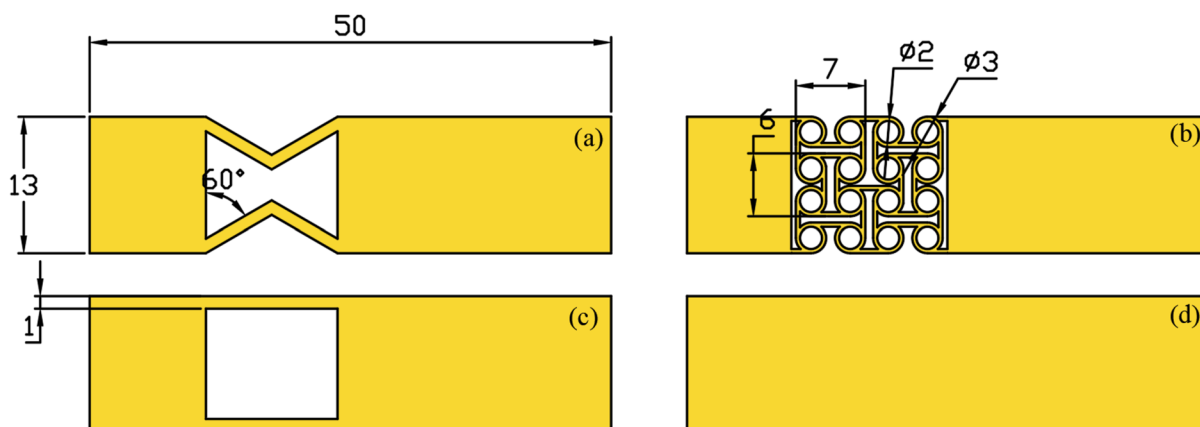


Fig. 5 Different substructures used in first case, a re-entrant, b anti-tetra-chiral, c rectangular, d plain

**Table 2** Resonance frequencies and optimum resistance values

Beam shape	Steel case		PLA case	
	Resonance frequency (Hz)	Optimum resistance (k $\Omega$ )	Resonance frequency (Hz)	Optimum resistance (k $\Omega$ )
Re-entrant	600	900	328	1600
Anti-tetra-chiral	450	1400	306	1600
Rectangular	800	700	336	1600
Plain	1300	3000	417	1400

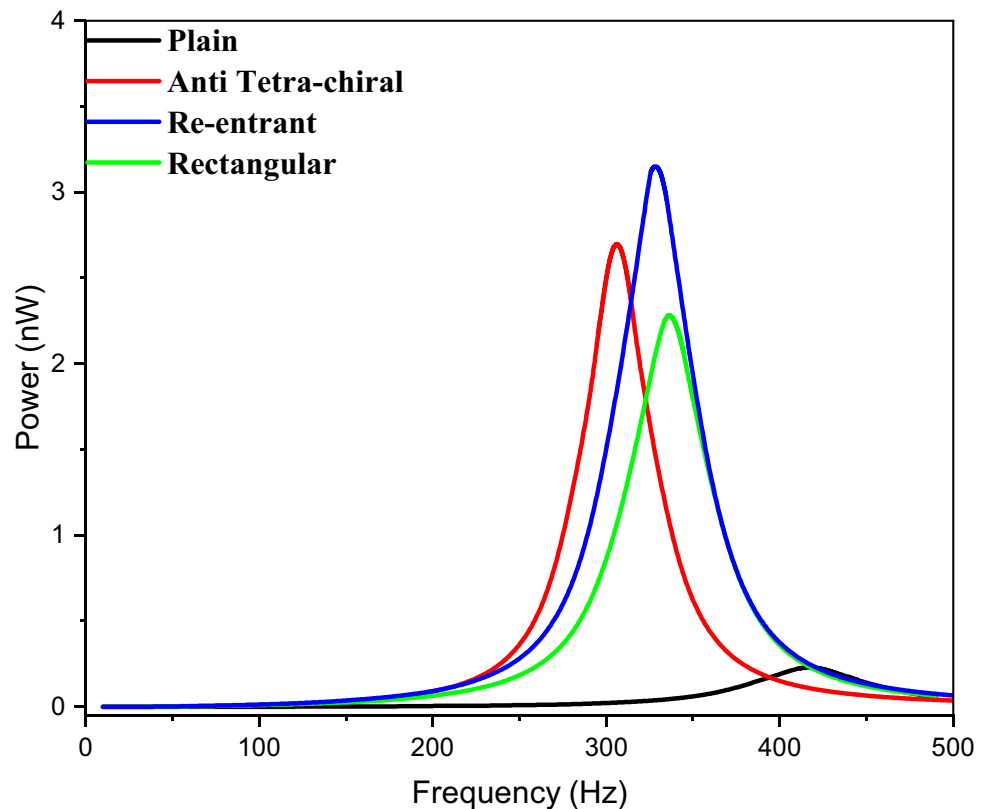
structures. Investigating the strain and stress distribution on piezoelectric materials can provide insight into the effect of auxetic structures on power gain.

The strain distribution in the x and y directions on the PVDF bonded on auxetic and non-auxetic cases were shown in Figs. 7 and 8. It is clear that all cases were generally in tension in x direction. When looking at the Fig. 7, strain in re-entrant case has a maximum value of 9 mikrostrain ( $\mu\text{S} = \mu\text{m}/\text{m}$ ) where plain one has only 2  $\mu\text{S}$ . On the other hand, 7  $\mu\text{S}$  of maximum strain was found for rectangular case. On the other hand, in y-direction, for rectangular and plain cases, the strain was in (–) range generally, and it was a bit uncertain (– and + range together) for re-entrant and anti-tetra-chiral cases. The average strain and stress values

for all cases can be seen in Table 4. Average strain in x direction was found to be 1.57  $\mu\text{S}$  for plain beam case, 5.12  $\mu\text{S}$  for rectangular and 5.63  $\mu\text{S}$  for re-entrant cases. It is increasing when using nonlinear geometry, however, the values are closed to each other for auxetic and non-auxetic rectangular geometries. On the other hand, the average strains in y direction –0.49  $\mu\text{S}$ , –1.33  $\mu\text{S}$  and –1.12  $\mu\text{S}$  for plain, rectangular and re-entrant cases, respectively. It can be seen that average strains in y direction were way lower than the strain in x direction and there is not a significant increase when auxetic structures were used. When looking at these values, it can be said that the effect of negative Poisson's ratio of auxetic structures was not very clear and the power increase was due to the effect stiffness decrease of the structures. The auxetic and non-auxetic geometries directly increased the strain in x-direction when compared to the plain structure. Also, when average stress values are calculated, the stresses

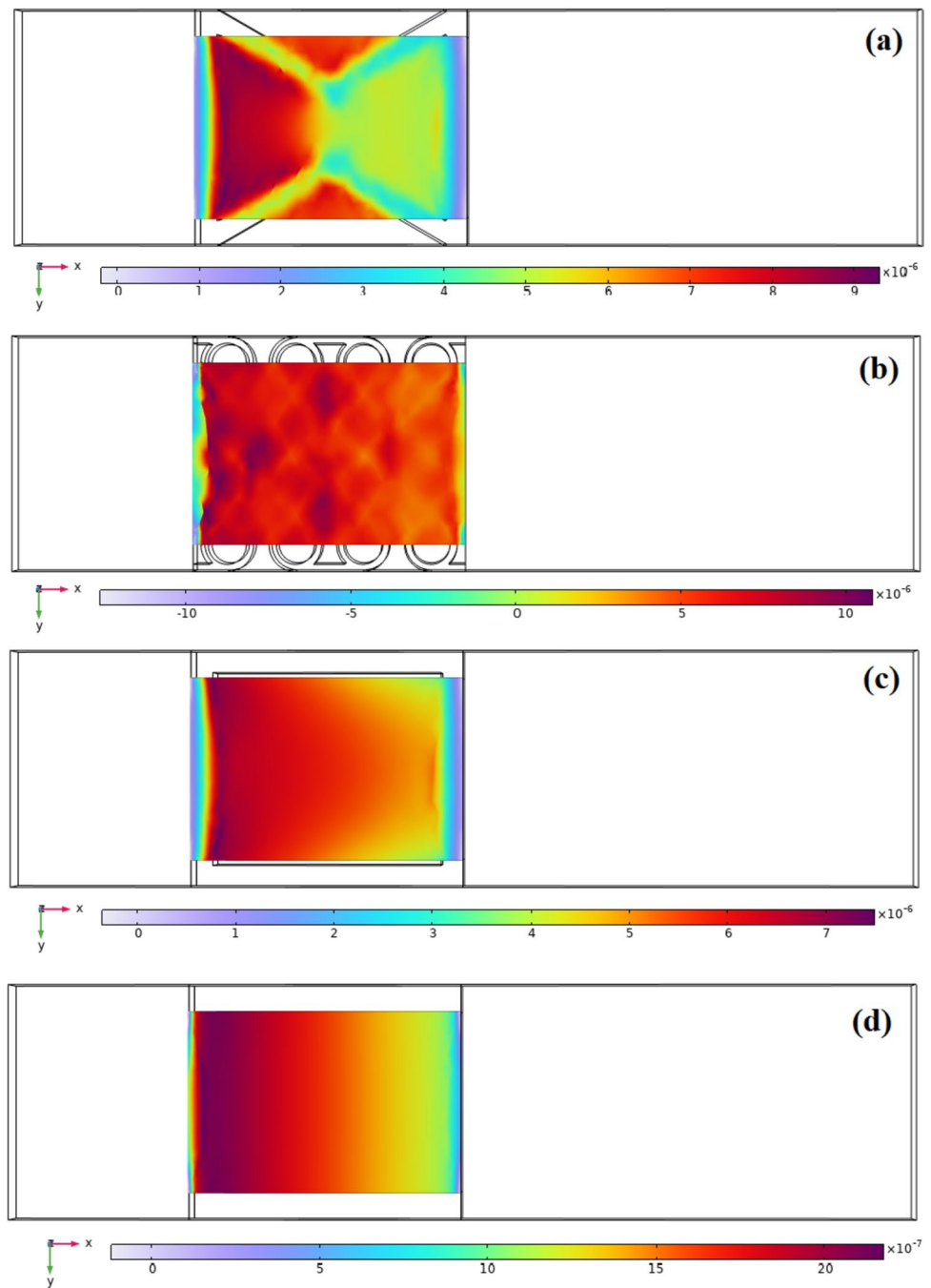
**Table 3** Maximum power responses of the structures for PLA case

Beam shape	Maximum power (nW)
Re-entrant	3.15
Anti-tetra-chiral	2.7
Rectangular	2.28
Plain	0.23

**Fig. 6** Power response of energy harvesters for different structures for PLA beam case



**Fig. 7** Strain distribution on PVDF in x-direction for PLA beam cases **a** re-entrant, **b** anti-tetra-chiral, **c** rectangular, **d** plain



in x-direction are very high compared to the y-direction stresses in all cases.

To further investigate, the stress distributions in x and y directions on the PVDF bonded on different cases were shown in Figs. 9 and 10. Maximum stress in x direction was found as 100 kPa for anti-tetra-chiral, around 30 kPa for rectangular and re-entrant cases and lower than 7 kPa for plain case. It should be mentioned that in anti-tetra-chiral case, the stress was not uniform and the maximum stress was occurred at some unique points. Average stress values can be seen in Table 4. Stresses in x and y direction was very low for plain

case, however, the values were closed to each other for rectangular and auxetic cases. In auxetic cases, it was expected that the stress in y-direction is very high when compared to non-auxetic structure. Therefore, it is hard to say that the negative Poisson's ratio of auxetic geometry really affected the power response of the harvester. Power boost compared to the plain structure was highly due to the area reduction and non-linear geometry. One reason for this can be inefficient energy transfer from substructure to the piezoelectric material due to low stiffness of the substructure material. In that case, substructure cannot bend the piezoelectric material

**Fig. 8** Strain distribution on PVDF in y-direction for PLA beam cases **a** re-entrant, **b** anti-tetra-chiral, **c** rectangular, **d** plain

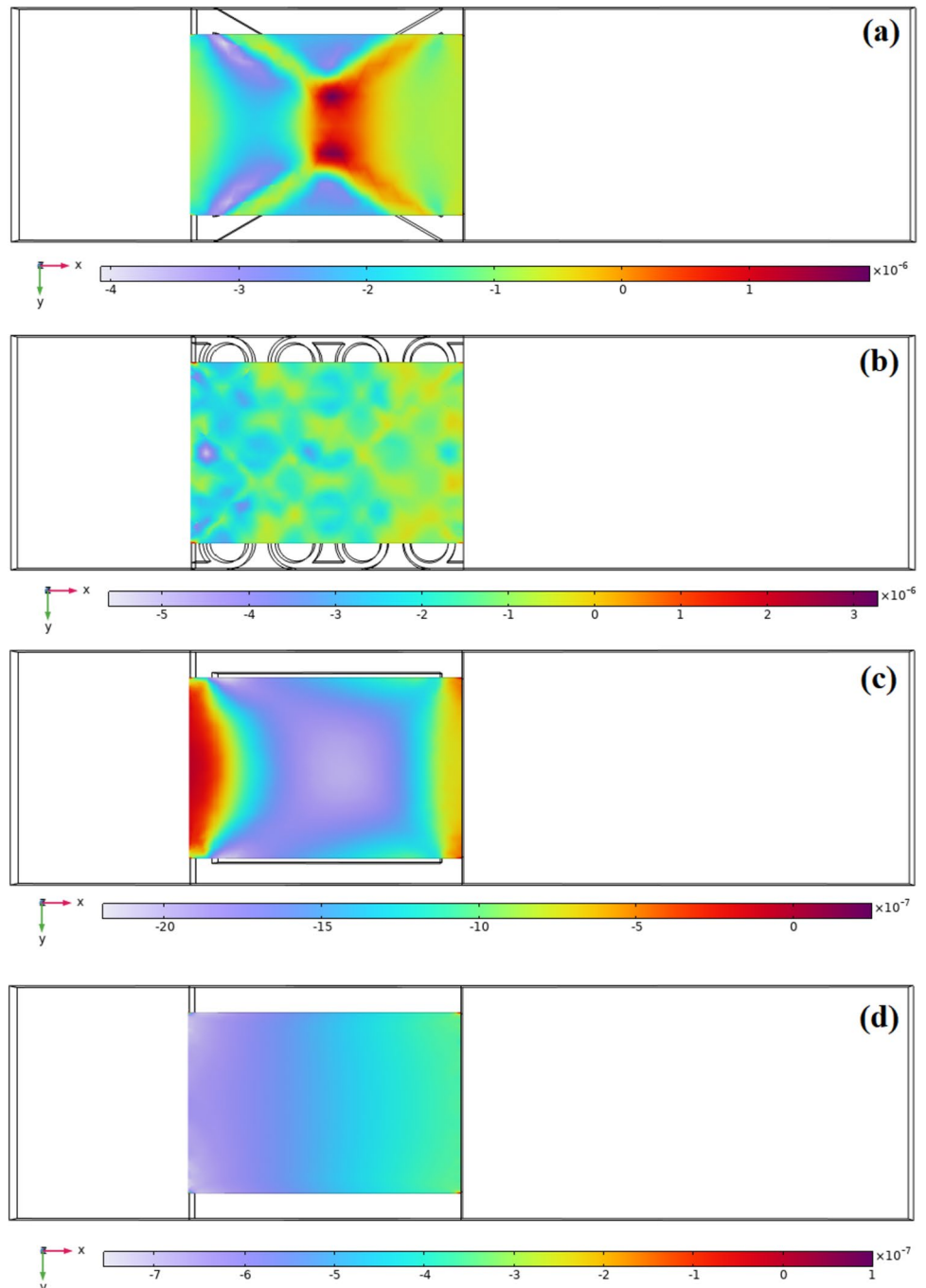


**Table 4** Average stress and strain values for different cases with PLA beam

	Average stress ( $\bar{\sigma}_{11}$ ) (Pa)	Average stress ( $\bar{\sigma}_{22}$ ) (Pa)	Average strain ( $\bar{S}_{11}$ ) ( $\mu\text{S}$ )	Average strain ( $\bar{S}_{22}$ ) ( $\mu\text{S}$ )
Re-entrant	16,300	3440	5.63	-1.12
Anti-tetra-chiral	16,300	2650	5.77	-1.43
Rectangular	14,400	2140	5.12	-1.33
Plain	4320	389	1.57	-0.49

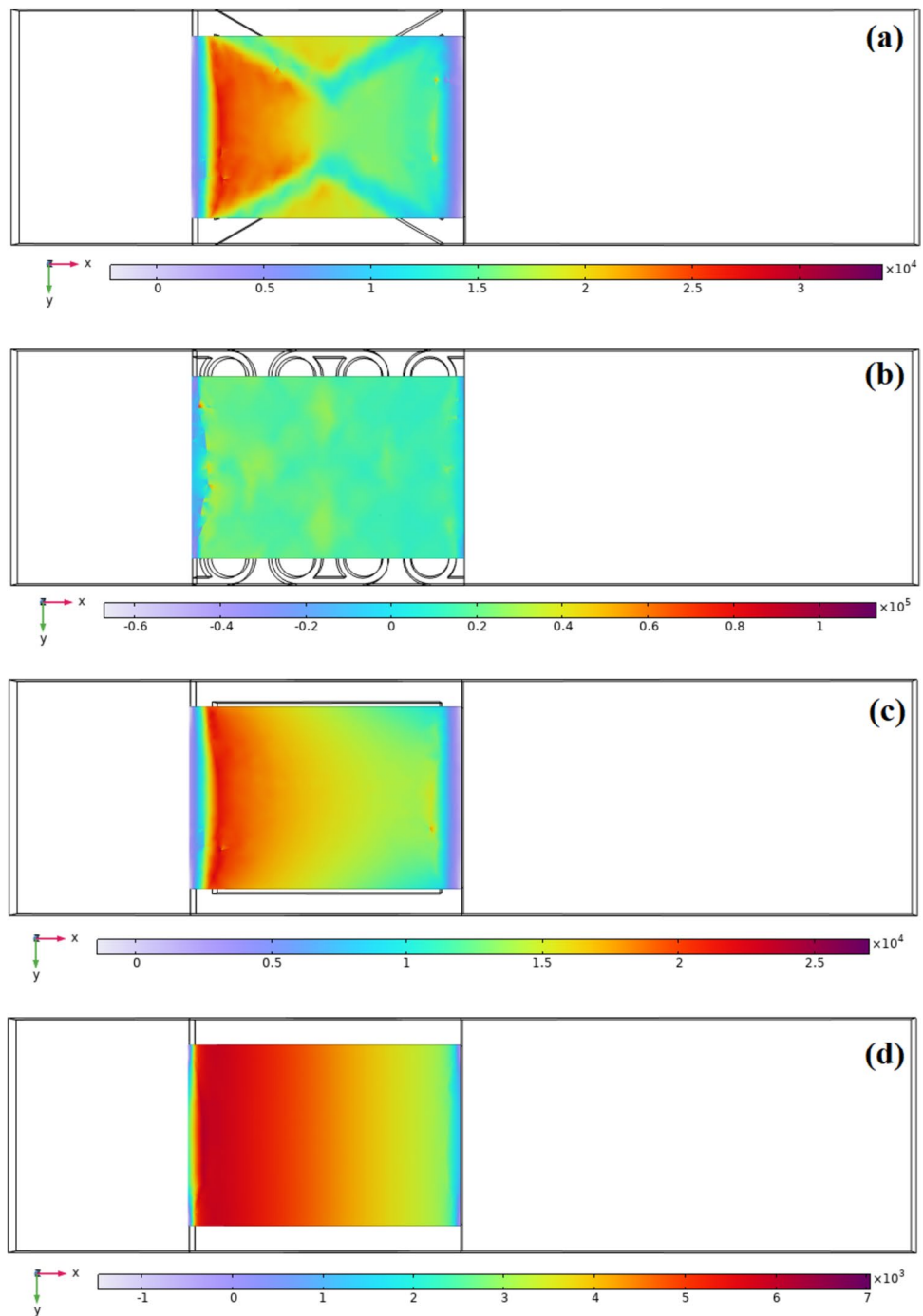
effectively and decreases the energy transfer from the beam to the piezoelectric material. It can be increased by using more stiff material in substructure such as steel.

**Steel Beam Case**

For a second case (Table 5), a steel substructure was used with same geometries. The stiffness of the steel beam is higher than the PLA beam due to the higher elasticity modulus. This was expected to increase the energy transfer from the beam to the piezoelectric material, in example,



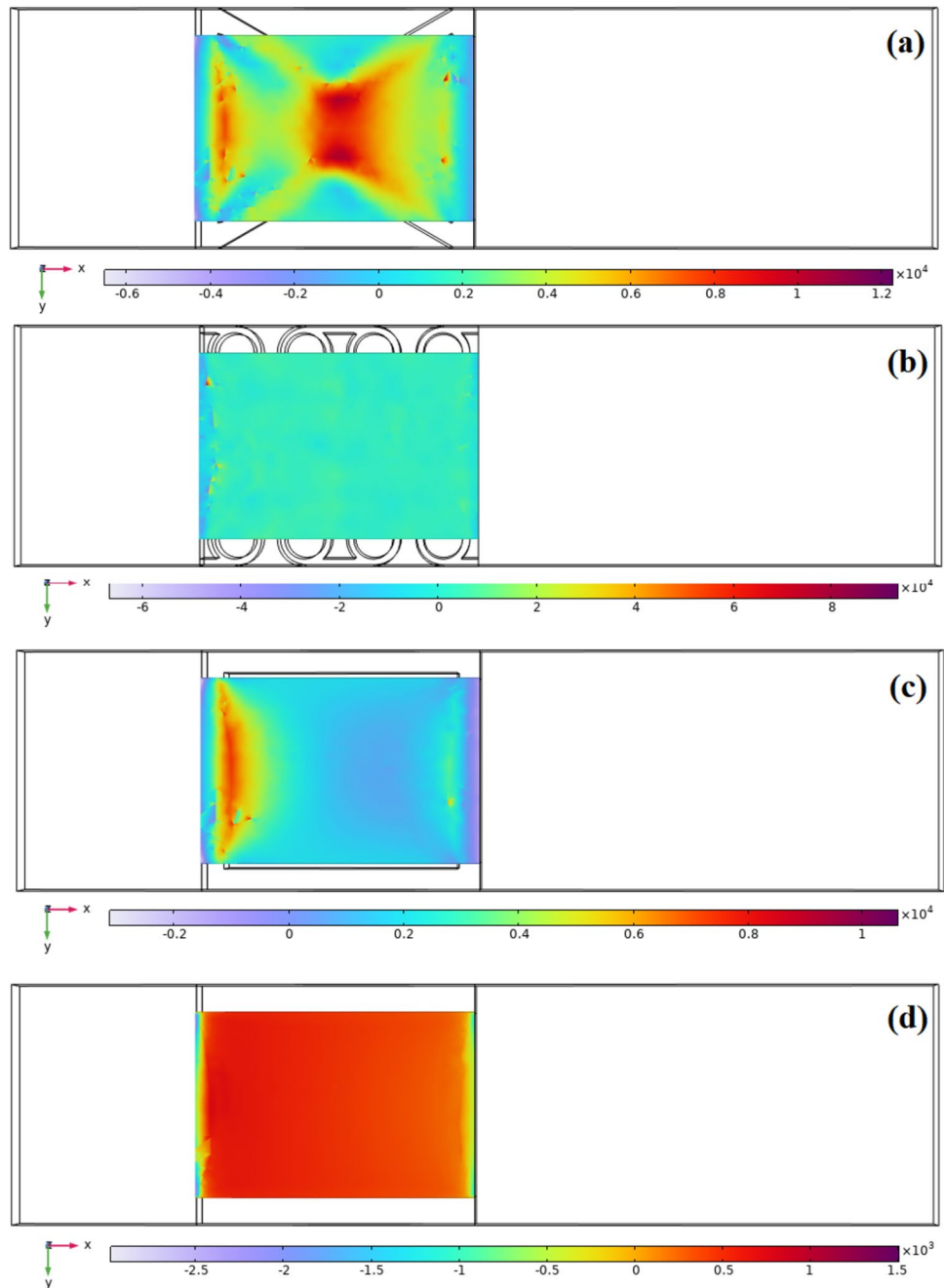
**Fig. 9** Stress distribution on PVDF in x-direction for PLA beam cases **a** re-entrant, **b** anti-tetra-chiral, **c** rectangular, **d** plain



steel beam can bend the piezoelectric material more effectively in this case. Power responses from different substructures can be seen in Fig. 11. Increase in power response due to the auxetic structures is clearer in this case. 1.1 nW of power was harvested by re-entrant case which was 1000 times of plain structure case and about 14 times of rectangular case. Also, anti-tetra-chiral case was 12 times of rectangular case. Even some of the harvested energy increase in auxetic structures could be due to the frequency

decrease in resonance frequency, there is still a significant increase due to the auxetic effect. Strain distributions in x and y directions were shown in Figs. 12 and 13, respectively. Maximum strain in x-direction for re-entrant case was around  $3.5 \mu\text{S}$  and it is  $20 \mu\text{S}$  for anti-tetra-chiral case. They were  $0.9 \mu\text{S}$  and  $0.08 \mu\text{S}$  for non-auxetic rectangular and plain cases, respectively. The more important part was in y-direction of the strain distribution. The maximum strain in y-direction occurred in PVDF were mostly in positive

**Fig. 10** Stress distribution on PVDF in y-direction for PLA beam cases **a** re-entrant, **b** anti-tetra-chiral, **c** rectangular, **d** plain



range for re-entrant and anti-tetra-chiral cases which shows the effect of negative Poisson’s ratio. The average strains and stresses occurred on PVDF can also be seen in Table 6.

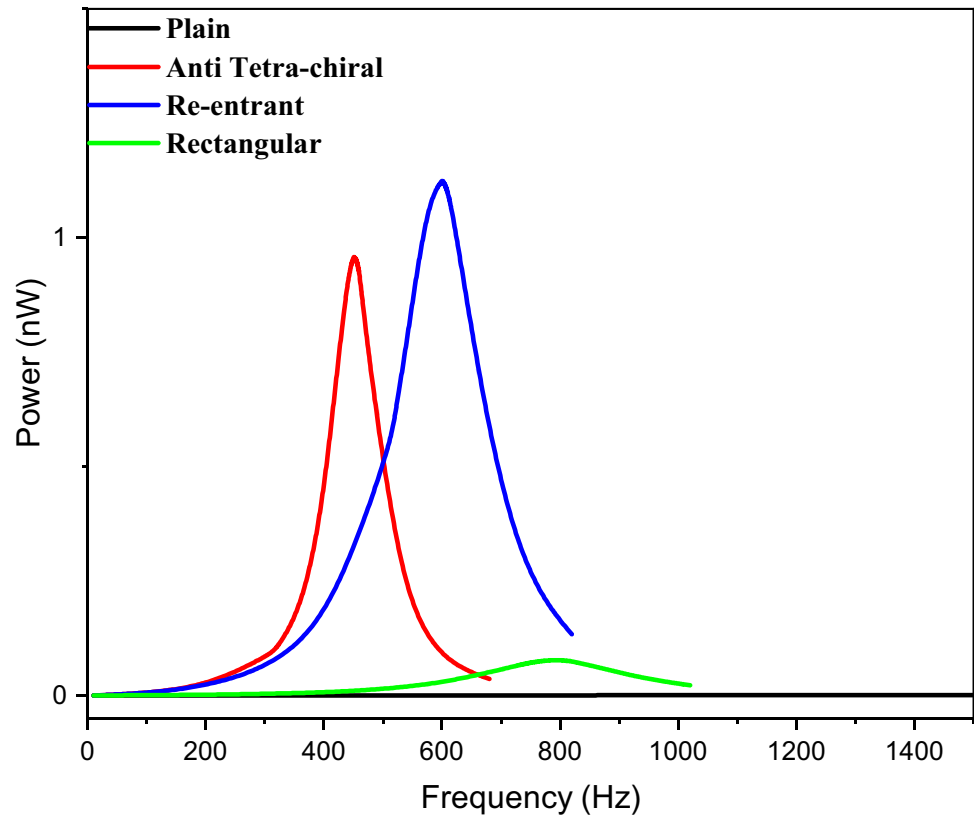
**Table 5** Maximum power responses of the structures for steel beam case

Beam shape	Maximum power (nW)
Re-entrant	1.12
Anti-tetra-chiral	0.96
Rectangular	0.075
Plain	0.001

It is clear that the only average positive strain in y-direction was obtained in re-entrant case. In other cases, the average strains in y-direction were in negative range. On the other hand, re-entrant structure gave very high x and y-direction stresses on PVDF when looking at the Table 6. The y-direction stress obtained by re-entrant geometry was closed to the x-direction strain which is a sign of the effect of the auxetic geometry.

For re-entrant case, the effect of auxetic behavior was very clear which gave the same sign in x and y direction increasing the power response. However, it was not valid for

**Fig. 11** Power response of energy harvesters for different structures with PVDF bonded on for steel beam case



anti-tetra-chiral substructure. This can be due to the highly nonuniform strain distribution in anti-tetra-chiral case. Therefore, it can be said that, negative Poisson's ratio is not enough alone to see the effect of auxetic structure, the geometry should be studied for each unique application (Table 6).

The use of auxetic structure in energy harvesting applications could improve the power response, however, this increase may not be significant when compared to the simple non-auxetic structures. To utilize the effect of negative Poisson's ratio, the stiffnesses of the beam and piezoelectric materials should be considered first to effectively stretch the piezoelectric materials in x and y directions. Otherwise, auxetic geometries only work as simple geometry with cavities and the power increase generally comes from the increase in displacement due to area reduction. On the other hand, auxetic geometries will be more effective in longitudinal vibrations due to the nature of the geometries and using them in transverse vibrations a bit harder as they can not show their performance effectively.

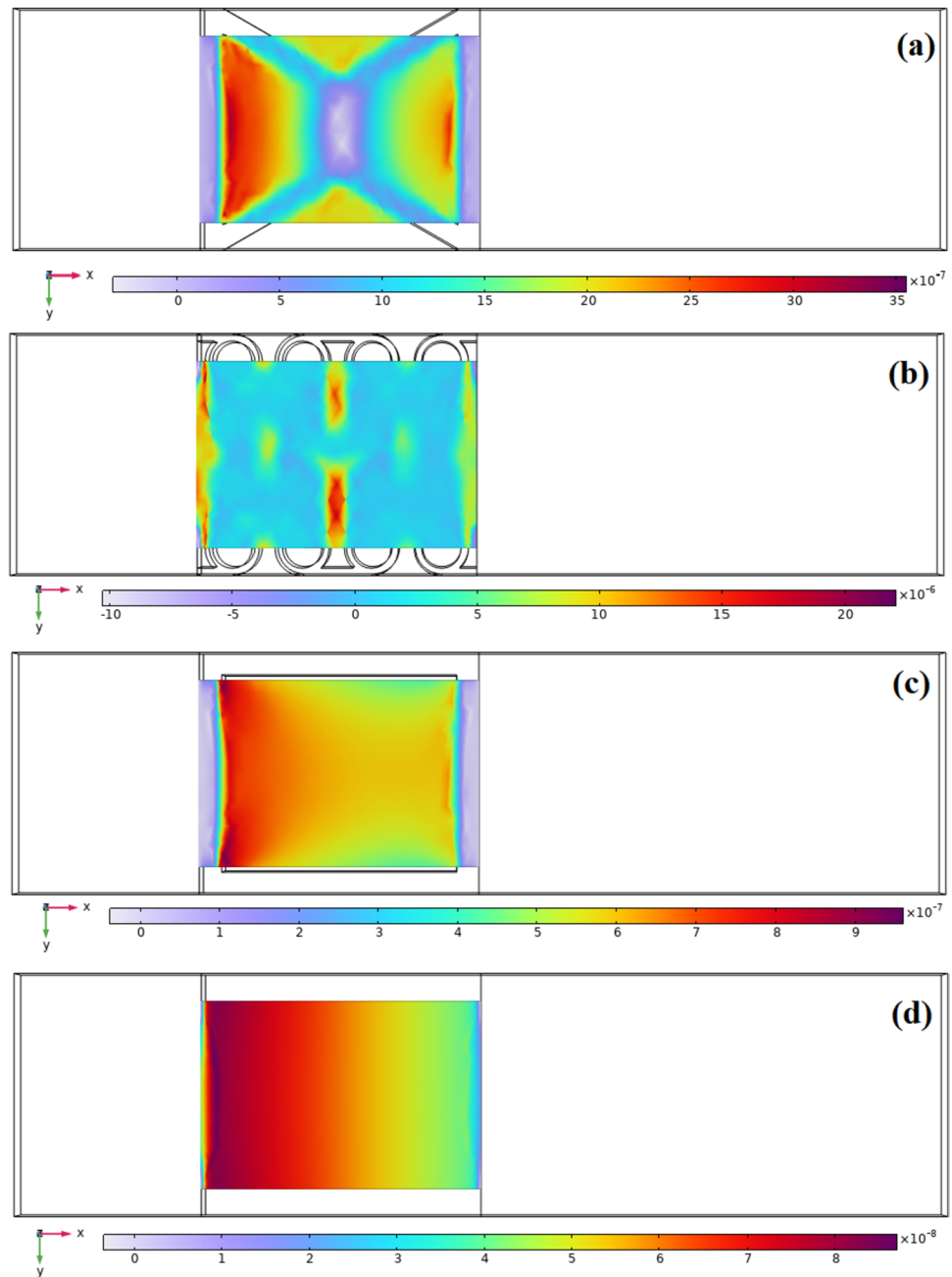
### Case-2: Energy Harvesting from New Shapes and Comparison to Auxetic and Plain Structures

New structures aiming to increase the strain in x-direction rather than focus on y-direction were offered in this case.

The new structures were inspired by re-entrant structure which was used in vertical direction and named as NS-A, NS-B and NS-C as shown in Fig. 14. NS-A was directly utilized by using one cell of re-entrant structure. NS-B was obtained by taking out some area from NS-A to decrease the stiffness and increase deflection. For NS-C, two cells of re-entrant structure were used. These structures aim to magnify the stretch of the beam in x direction rather than changing the direction of the strain in y-direction. Because the strain in x-direction is very high compared to the strain in y-direction for bending motion of the beam, increasing the strain in x-direction are expected to affect the harvested energy more. These harvesters were analyzed under identical conditions as those in Case 1, and their maximum power responses were compared to the results of the re-entrant geometry, which exhibited the best performance in previous part.

The resonance frequencies and optimum resistance values were given in Table 7. It can be seen that minimum resonance frequency was achieved by NS-B which has maximum area reduction and lower stiffness due to its geometry. Figure 15 shows the power responses obtained from the offered structures when PLA was used as beam material under optimum external resistances. It is obvious from the figure that maximum power was gained with the use of NS-B. All the new structures harvested more power from

**Fig. 12** Strain distribution on PVDF in x-direction for steel beam cases **a** re-entrant, **b** anti-tetra-chiral, **c** rectangular, **d** plain



re-entrant structure. The maximum power values can be seen in Table 8. Power increase is nearly 25% for NS-A compared to the re-entrant case and it is 17 times of plain case. When looking at the NS-B and NS-C, there is a nearly 5 times and 3 times increase in power when compared to the re-entrant case. When compared to the plain beam case, this increase reaches nearly 65 times for NS-C case.

The same analysis was made using steel as beam material and the power responses can be seen in Fig. 16 and Table 9. It can be seen that the maximum harvested was achieved by

NS-B giving nearly 42 nW. Power response of NS-A is very low compared to others in this case with a 0.12 nW, however, all the new geometries gave very high power responses compared to the plain beam (Table 9).

In the last part of the study, an experimental study was performed to show the effect of the new design in power generation and the results were compared to the FEA results. Here, 3D printed PLA based substructure was used with PVDF bonded on both sides.

**Fig. 13** Strain distribution on PVDF in y-direction for steel beam cases **a** re-entrant, **b** anti-tetra-chiral, **c** rectangular, **d** plain

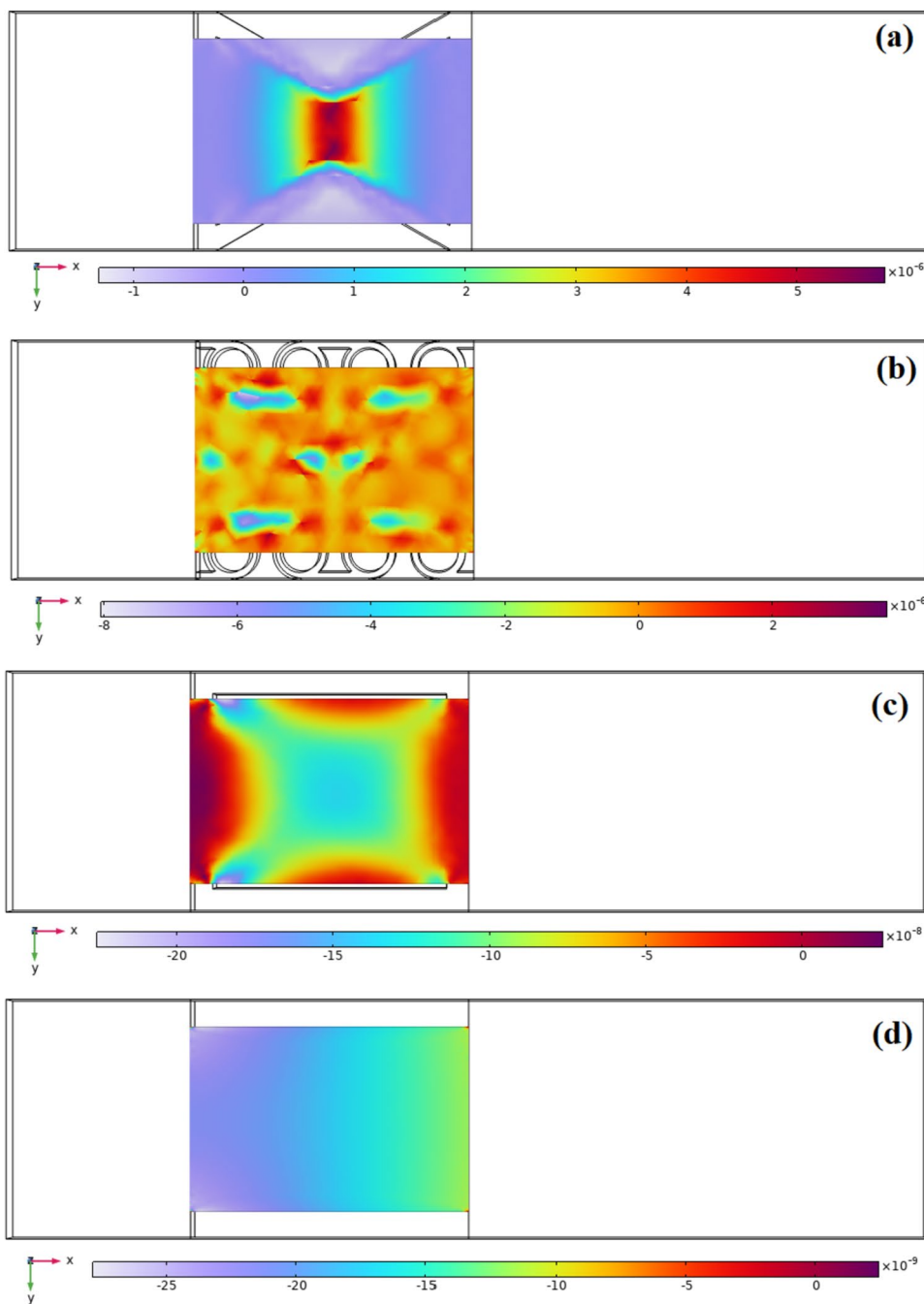


**Table 6** Average stress and strain values for different cases with steel beam

	Average stress ( $\bar{\sigma}_{11}$ )	Average stress ( $\bar{\sigma}_{22}$ )	Average strain ( $\bar{S}_{11}$ )	Average strain ( $\bar{S}_{22}$ )
Re-entrant	5100	3600	1.39	0.59
Anti-tetra-chiral	7550	1760	2.59	-0.45
Rectangular	1550	422	0.52	-0.07
Plain	163	17.4	0.059	-0.017

As the experimental set-up is only capable of applying a maximum external load of 1 M $\Omega$ , it was used as load in this case. The results were given in Fig. 17 comparing the results to the FEA. Resonance frequencies were found to be at 355 and 300 Hz in experiments for re-entrant and NS-A structures, respectively. When, they are compared to the FEA results of these structures which were 273 and 328 Hz, it can be seen that there is a difference below 10%. This result could be due to the non-perfect fixture of the beam to the shaker. The maximum power values are lower in the FEA cases due to the same reason as well as solution

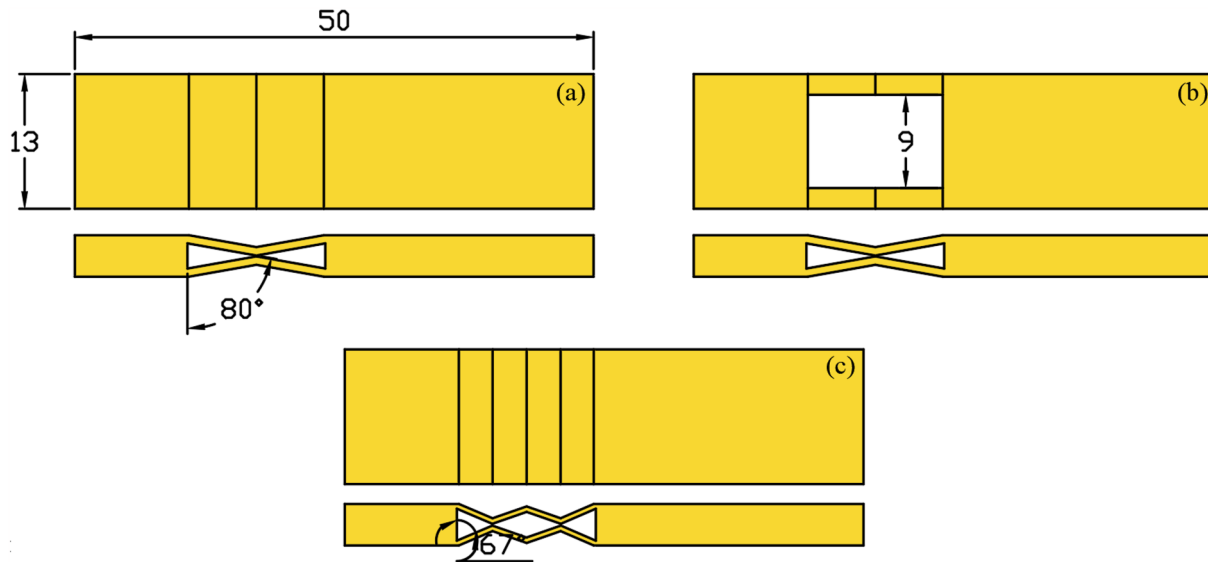


Fig. 14 New structures offered a NS-A, b NS-B, c NS-C

**Table 7** Resonance frequencies and optimum resistance values for new structures

Beam shape	Steel case		PLA case	
	Resonance frequency (Hz)	Optimum resistance (k $\Omega$ )	Resonance frequency (Hz)	Optimum resistance (k $\Omega$ )
NS-A	666	800	273	2000
NS-B	215	2500	122	2500
NS-C	360	2000	190	3000

step difference in FEA and experiments. Maximum powers were found to be 2.9 and 3.33 nW for re-entrant and NS-A structures, respectively, in experiments. There is a difference below 8% between these values and FEA results which are 2.75 and 3.05 nW for re-entrant and NS-A structures, respectively. On the other hand, the trends are very closed to each other and the differences in FEA and experiment nearly same in all cases and they are in acceptable rates. Therefore, it can be said that FEA results matched well with experiments.

There is a 15% increase in power when compared to the re-entrant case. These results show that, the new offered structure perform better in this case from an auxetic structure and plain structure.

## Conclusion

Despite the huge potential for application of piezoelectric energy harvesters, typical harvested powers, however, remain in low range, and further effort is therefore required to boost these values towards a more useful magnitude. This study aims to investigate the potential boosting effect of the geometry modification of the substructure on harvested power. First, auxetic shaped beams were analyzed for their contribution to the energy production from different piezoelectric materials under transverse vibrations which is a popular research area in recent days. The results have shown that, increasing strain in y-direction is difficult for transverse vibrations and the stiffness of substructure and piezoelectric material effects this phenomenon. For PLA case, there was 13 times increase in power response when compared to the plain beam. However, this increase was not due to the auxetic effect (negative Poisson's ratio), rather, it was due to the area reduction of the geometry as can be seen from average strain values. Moreover, this increase in power was also mostly achieved by a non-auxetic rectangular structure which was nearly 10 times of plain case. On another case, steel was used as substructure material which has higher stiffness compared to the PLA. In this case, the advantage of negative Poisson's ratio was clearer, in which, re-entrant structure harvested nearly



**Fig. 15** Power response of offered structures with PVDF bonded on for PLA beam case

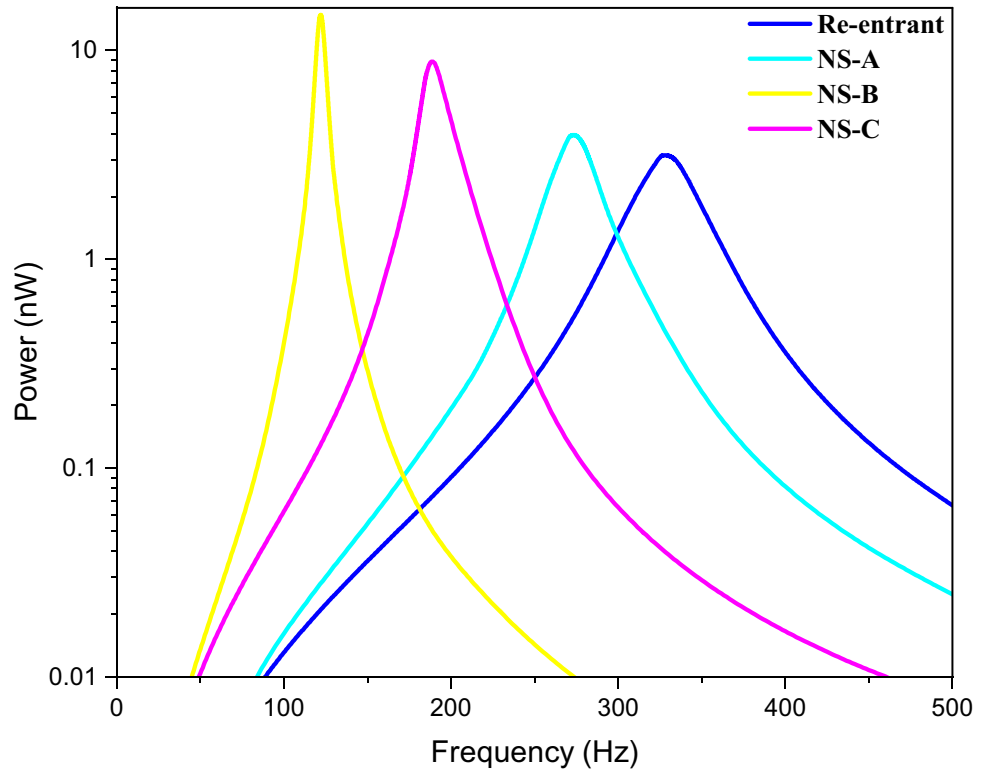


**Table 8** Maximum power responses of the structures for PLA case

Beam shape	Maximum power (nW)
NS-A	3.94
NS-B	15
NS-C	10.3
Re-entrant	3.15
Plain	0.23

**Table 9** Maximum power responses of the structures for steel case

Beam shape	Maximum power (nW)
NS-A	0.12
NS-B	42.5
NS-C	3.35
Re-entrant	1.12
Plain	0.001

15 times of rectangular geometry and 1000 times of plain one. Also, average strain in y-direction turned into positive range, as expected from an auxetic structure. However, the values were lower than that of the PLA case, as the increase in stiffness reduced the vibration amplitude and consequently strain levels. For the second part of the

study, new structures inspired by re-entrant geometry was utilized aiming to increase the strain in x-direction, rather focusing on strain in y-direction. These geometries outperformed the plain beam and re-entrant structure in PLA and steel cases. Nearly 5 times of re-entrant case and 65 times of plain case was achieved by NS-B structure for PLA beam and NS-A and NS-C also performed better from compared the structures. In steel case, the increase was better reaching 45 times of re-entrant case. Finally, some of the structures were produced and experimentally validated in the last part of the study. As final remarks for this study, it can be said that utilizing auxetic geometries can increase power response in energy harvesting applications with transverse vibrations, however, this increase is affected by the stiffness match between piezoelectric material and substructure. On the other hand, using vertical re-entrant geometries in energy harvesters, power can be increased in significantly comparing to the auxetic geometries. Even the increase in power can be unique to the applied case, the idea of using vertical re-entrant geometries can give inspiration on further studies. Also, these structures can be modified for desired application by changing dimensions of the geometry. Different structures give unique performances in different cases and there is not an optimum geometry for all cases. However, new shapes offered in this study have a potential for increased power response for piezoelectric energy harvesting applications when they are used considering

**Fig. 16** Power response of offered structures with PVDF bonded on for steel beam case

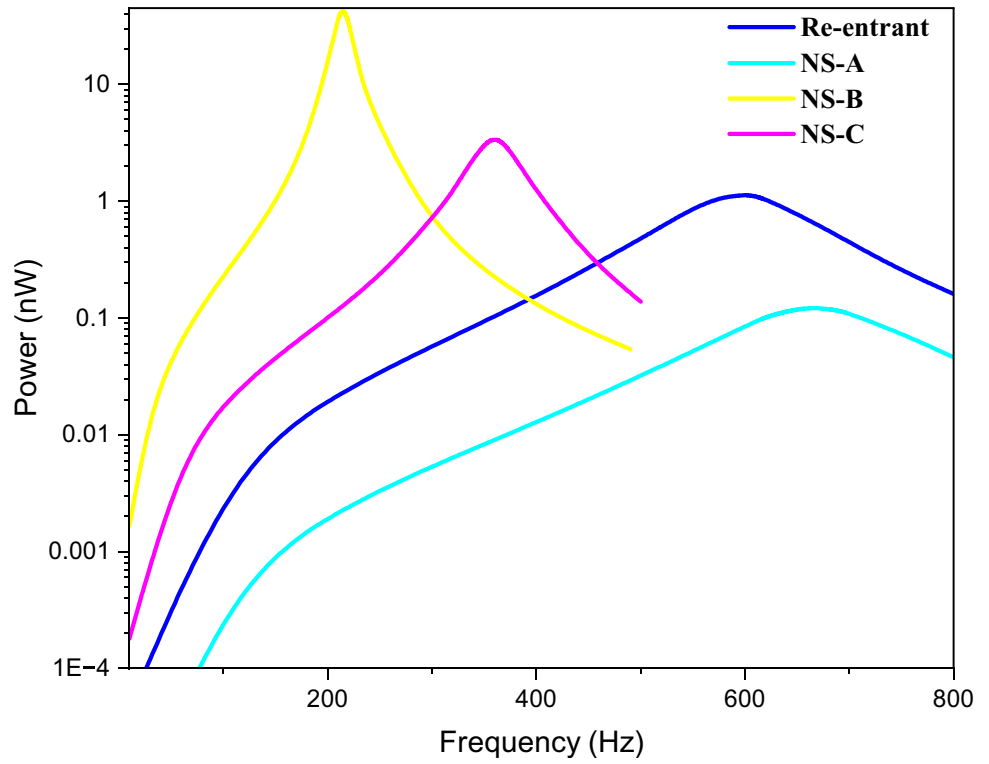
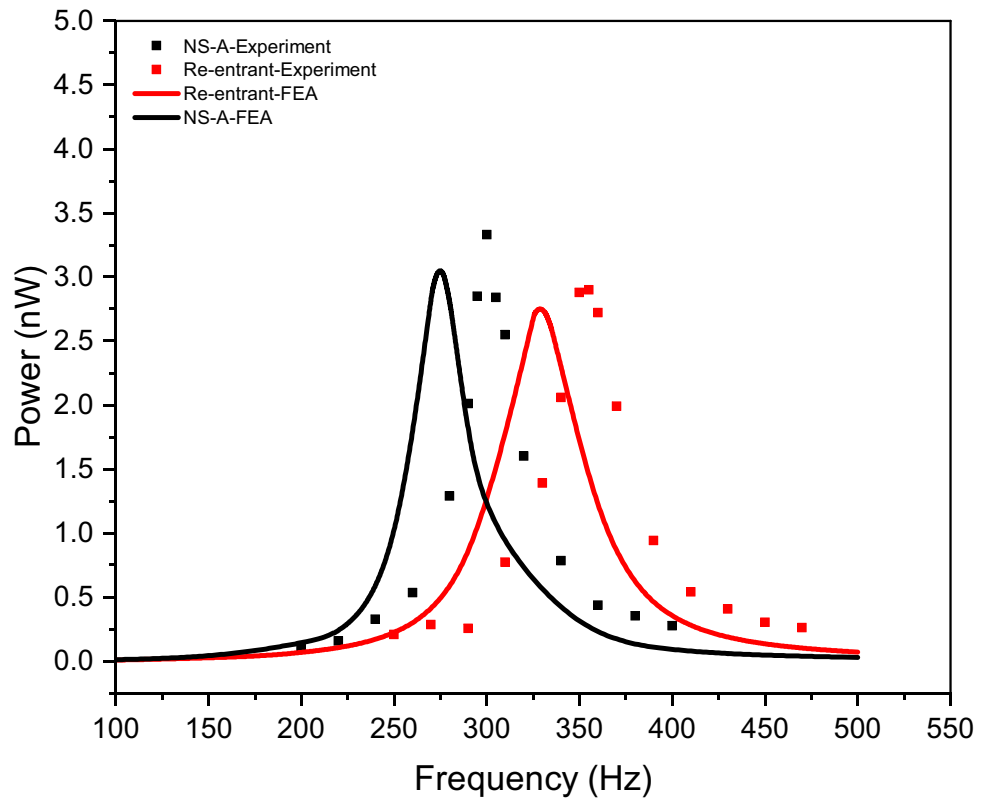


**Fig. 17** Power responses for the structures in Case-2, comparing experimental data and FEA



their stiffnesses and natural frequencies of the desired application.

**Funding** Open access funding provided by the Scientific and Technological Research Council of Türkiye (TÜBİTAK).

## Declarations

**Conflict of interest** All authors declare that they have no conflicts of interest.

**Open Access** This article is licensed under a Creative Commons Attribution 4.0 International License, which permits use, sharing, adaptation, distribution and reproduction in any medium or format, as long as you give appropriate credit to the original author(s) and the source, provide a link to the Creative Commons licence, and indicate if changes were made. The images or other third party material in this article are included in the article's Creative Commons licence, unless indicated otherwise in a credit line to the material. If material is not included in the article's Creative Commons licence and your intended use is not permitted by statutory regulation or exceeds the permitted use, you will need to obtain permission directly from the copyright holder. To view a copy of this licence, visit <http://creativecommons.org/licenses/by/4.0/>.

## References

1. Feenstra J, Granstrom J, Sodano H (2008) *Mech Syst Signal Process* 22:721–734
2. Abohamer MK, Awrejcewicz J, Amer TS (2023) *Nonlinear Dyn* 111(9):8217–8234
3. Proto A, Penhaker M, Bibbo D, Vala D, Conforto S, Schmid M (2016) *Sensors* 16:524
4. Abohamer MK, Awrejcewicz J, Starosta R, Amer TS, Bek MA (2017) *Appl Sci* 11(18):8658
5. Abohamer MK, Awrejcewicz J, Amer TS (2023) *Alex Eng J* 63:377–397
6. Erturk A, Inman DJ (2011) *Piezoelectric energy harvesting*. Wiley, Hoboken
7. Roscow JI, Lewis RWC, Taylor J, Bowen CR (2017) *Acta Mater* 128:207
8. Szewczyk PK, Gradys A, Kim SK, Persano L, Marzec M, Kryshtal A, Busolo T, Toncelli A, Pisignano D, Bernasik A, Kar-Narayan S, Sajkiewicz P, Stachewicz U, *Appl ACSACS* (2020) *Mater Inter* 12(11):13575
9. Zhang Q, Cai W, Li Q, Gao R, Chen G, Deng X, Wang Z, Cao X, Fu C (2019) *J Alloy Compd* 794:542
10. Zeyrek Ongun M, Oguzlar S, Doluel EC, Kartal U, Yurddaskal M (2020) *J Mater Sci Mater Electron* 31:1960–1968
11. Liang J, Liao WH (2010) *Proc SPIE* 7643:181–192
12. Kong NA, Ha DS, Erturk A, Inman DJ (2010) *J Intel Mat Syst Str* 21:1293
13. Wang Q, Li S, Oh JAS, Wu T (2020) *Mater Technol* 35:650
14. Zhou X, Parida K, Chen J, Xiong J, Zhou Z, Jiang F, Xin Y, Magdassi S, Lee PS (2023) *Adv Energy Mater* 13(34):2301159. <https://doi.org/10.1002/aenm.202301159>
15. Szymon W, Rybicki J (2022) *Comp Mater Sci* 201:110914
16. Mustahsan F, Khan SZ, Zaidi AA, Alahmadi YH, Mahmoud ERI, Almohamadi H (2022) *Materials* 15:8022
17. Ravanbod M, Ebrahimi-Nejad S (2023). *Mech Adv Mater Struct*. <https://doi.org/10.1080/15376494.2023.2280997>
18. Man D, Zhang Y, Xu G, Kuang X, Xu H, Tang L, Han T (2023) *Alex Eng J* 76:153–165
19. da Silveira ARG, Daniel GB (2022) *Mech Syst Signal Process* 166:108404
20. Ferguson WJG, Kuang Y, Evans KE, Smith CW, Zhu M (2018) *Sensor Actuat A-Phys* 282:90
21. Chen K, Gao Q, Fang S, Zou D, Yang Z, Liao WH (2021) *Appl Energ* 298:117274
22. Eghbali P, Younesian D, Moayedizadeh A, Ranjbar M (2020) *Sci Rep* 10:16338
23. Radhika SSB, Pandurangan V (2022) *Smart Mater Struct* 31:105015
24. Chen K, Fang S, Gao Q, Zou D, Cao J, Liao WH (2022) *Appl Phys Lett* 120:103901
25. Li Q, Kuang Y, Zhu M (2017) Auxetic piezoelectric energy harvesters for increased electric power output. *Aip Adv* 7(1):015104
26. Eghbali P, Younesian D, Farhangdoust S (2020) *Int J Energ Res* 44:1179
27. Farhangdoust S, Georgeson G, Ihn JB, Chang FK (2020) *Smart Mater Struct* 30:015037
28. Li Q, Kuang Y, Zhu M (2017). *Aip Adv*. <https://doi.org/10.1063/1.4974310>

**Publisher's Note** Springer Nature remains neutral with regard to jurisdictional claims in published maps and institutional affiliations.